Nanomed. J. 9(4):319-327, Autumn 2022

RESEARCH PAPER

Synthesis and evaluation of anti-inflammatory properties of hydroxyapatite nanoparticles in an experimental model of colitis

Fereshteh Asgharzadeh [1, 2#], Alireza Hashemzadeh [1#], Moein Eskandari [3], Atieh Yaghoubi [4, 2], Niloufar Naghibzadeh [1], Asma Mostafapour [5], Seyedeh Elnaz Nazari [1], Ghazaleh Khalili-Tanha [5, 6], Ayda Bakhshi [2], Saman Soleimanpour [4], Amir Avan [5, 6, 7], Seyed Mahdi Hassanian [3], Majid Rezayi [5*], Majid Khazaei [1, 5*]

[1]Department of Physiology, Faculty of Medicine, Mashhad University of Medical Sciences, Mashhad, Iran
[2]Student Research Committee, Faculty of Medicine, Mashhad University of Medical Sciences, Mashhad, Iran
[3]Department of Clinical Biochemistry, Faculty of Medicine, Mashhad University of Medical Sciences, Mashhad, Iran
[4]Department of Microbiology and Virology, School of Medicine, Mashhad University of Medical Sciences, Mashhad, Iran
[5]Metabolic Syndrome Research Center, Mashhad University of Medical Sciences, Mashhad, Iran
[6]Medical Genetics Research center, Faculty of Medicine, Mashhad University of Medical Sciences, Mashhad, Iran
[7]Basic Sciences Research Institute, Mashhad University of Medical Sciences, Mashhad, Iran

ABSTRACT

Objective(s): Ulcerative colitis (UC) is a chronic large intestinal condition, for treatment and prevention of which sulfasalazine (SSZ) is used. It functions by helping to reduce inflammation and other disease symptoms within the bowels, but this drug has many side effects. Various novel paths for UC treatment are being studied to solve the difficulties associated with present treatments and to design a more targeted therapy. Hydroxyapatite nanoparticles (HAP-NPs) form an inorganic portion of the natural bone and are primarily used in tissue engineering due to their anti-inflammatory and anti-toxicity character. This study aimed to investigate the anti-inflammatory character of sulfasalazine-containing HAP (SSZ-HAP-NPs) as a potential therapeutic agent.

Materials and Methods: The therapeutic efficacy of SSZ-HAP-NPs compared with SSZ as a standard drug was examined in a mouse model of colitis by induction of DSS for 7 days. Drugs were given on the third day and continued for seven days. Colonic mucosal inflammation was evaluated clinically, biochemically, and histologically.

Results: Our results showed that SSZ-HAP-NPs clinically improved signs/symptoms more than SSZ, however, it was not statistically significant (P>0.05). Also, SSZ-HAP-NPs diminished histopathological evidence of injury, by decreasing inflammatory responses and balancing oxidative/anti-oxidative markers in colonic tissues (P>0.05).

Conclusion: SSZ-HAP-NPs could be more effective than SSZ as standard drug in some laboratory and clinical signs/symptoms and side effects in colitis and this could be a good strategy for future studies to use nanoparticles with more anti-inflammatory effects to develop the efficiency of standard drugs in colitis treatment.

Keywords: *Colitis; Hydroxyapatite; Inflammation; Nanoparticles*

How to cite this article
Asgharzadeh F, Hashemzadeh AR, Eskandari M, Yaghoubi A, Naghibzadeh N, Mostafapour A, Nazari SE, Khalili-Tanha Gh, Bakhshi A, Soleimanpour S, Avan A, Hassanian SM, Rezaei M, Khazaei M. Entrapped chemically synthesized gold nanoparticles combined with polyethylene glycol and Chloroquine diphosphate as an improved antimalarial drug. Nanomed J. 2022; 9(4):319-327. DOI: 10.22038/NMJ.2022.65906.1691

INTRODUCTION

Inflammatory bowel diseases (IBD) are chronic inflammatory diseases of the digestive tract, consisting of ulcerative colitis (UC) and Crohn's disease (CD) [1]. UC involves the rectal and descending colon, and CD can include some portion of the mouth-to-anus digestive tract. The cause of IBD is not clear, although many factors are believed to be linked to the production of

* *Corresponding authors: Emails: Rezaeimj@mums.ac.ir; Khazaeim@mums.ac.ir*
Note. This manuscript was submitted on Jun 4, 2022; approved on August 16, 2022
# These authors contributed eqully to this work

IBD, such as genetic and environmental factors, immunological factors, microbial pathogens, and dietary antigens [1]. IBD is described by excessive secretion of pro-inflammatory markers caused by the extreme beginning of common inflammatory signaling, such as tumor necrosis factor-alpha (TNF-α), interleukin (IL)-1, IL-6, and IL-12, and by an imbalance of pro-and anti-inflammatory tissue marker levels [2]. For the treatment of inflammatory bowel diseases, drugs such as corticosteroids, sulfasalazine (SSZ), 5-aminosalicylates (5-ASA), and immunosuppressive drugs are commonly utilized [3]. Nevertheless, not all patients respond to these treatments. In addition, deleterious adverse effects are frequently correlated with the pharmacological approach. Taken along with their high economic expense, presently existing treatments desperately need a better alternative.

For local disorders affecting the colon, targeted medicine delivery is a hot topic of research, as it increases clinical effectiveness and requires localized therapy, thus reducing systemic toxicity [4]. For the treatment of IBD, like UC and CD, selective release of therapeutics to the colon is mainly beneficial [4]. Advances like oral drug delivery have greatly increased the colorectal bioavailability of medications; however, provisions need to be made about the altered physiology of the digestive tract involved with digestive tract inflammation for a drug to have therapeutic effectiveness during illness [5]. In oral drug formulation design, nanotechnology was used as a strategy to further increase the absorption of diseased tissue within the colon [5].

Hydroxyapatite nanoparticles (HAP-NPs) are an inorganic component of the natural bone, and owing to their bioactivity, osteoconductivity, biocompatibility, anti-inflammatory, and anti-toxicity properties are mainly used in tissue engineering [6]. Current anti-inflammatory human health evidence for HAP-NPs, however, is restricted and only insufficient findings from basic research have been released. Since nanostructured materials typically perform much better than their bigger particle-sized complements because of their particular physical and chemical properties, HAP-NPs are also supposed to have improved bioactivity than coarser crystals [7]. Therefore, this study was conducted to examine the beneficial role of SSZ-HAP-NPs in alleviating colitis induced by DSS in animal models.

MATERIALS AND METHODS

Animals

C57Balb/6 mice (Male) were purchased from Mashhad University of Medical Science (MUMS) animal breeding facility. With access to regular chow and autoclaved drinking water *ad libitum*, mice were individually caged. Animals with a 12-hr day/night light period were housed at a standard temperature and humidity. During an acclimatization period of 7 days before being used in the tests, individual body weights (BW) were measured regularly. The Animal Ethics Committee of MUMS approved all procedures.

Instruments used

Infrared (IR) spectrum was characterized on KBr disk using a Fourier transform (FT)-IR JASCO FT-IR-460 spectrometer instrument. The X-ray powder diffraction (XRD) analysis of nanoparticles was collected by Philips PW1730 diffractometer. The transmission electron microscopy (TEM) was characterized using JEOL at 300 kV (JEM2100F) to analyze the morphology and size of synthesized HAP nanostructure.

Experimental design and drug treatment

C57Balb/6 male mice with 18–20 g (average weight) were randomly separated into four groups (n=6/group): controls without DSS received usual drinking water, DSS treatment (colitis), DSS + SSZ treatment (SSZ), and DSS + SSZ-HAP-NPs treatment

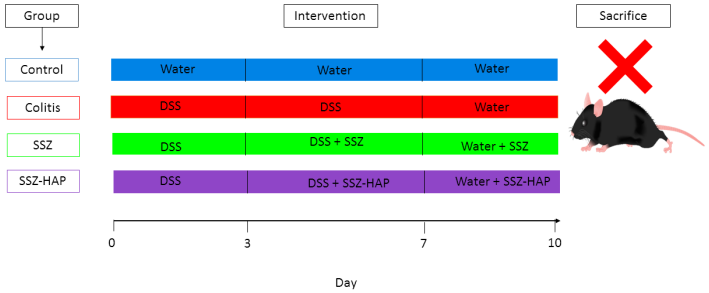

Fig. 1. Experimental design for administration of DSS and SSZ-HAP in C57BL/6J mice model of colitis

Table 1. DAI scoring parameters

Disease activity index (DAI)				
Score	Rectal bleeding	Stool consistency	Rectal prolapse	Lose weight
0	None	Normal	None	<5%
1	Red	Soft	Sign of prolapse	5-10%
2	Dark red	Very soft	Clear prolapse	10-15%
3	Gross bleeding	Diarrhea	Extensive prolapse	>15%

(SSZ-HAP). UC was induced by administering 1.5% DSS (molecular weight-40,000 KDa) (Sigma, USA) in consumption water to all groups except control, continuously over seven days from 0–7 days. SSZ (Tehran Daru, IRAN) was administered orally (p.o) at a dose of 100 mg/kg/day and DSS + SSZ-HAP-NPs were administered p.o at a dose of 100 mg/kg/day for a 7-day treatment period (from day 3-10) (Fig. 1) [8]. Body weight (BW), diarrhea, rectal bleeding, and prolapse were evaluated every day throughout the study. After ten days, the animals were sacrificed by cervical dislocation, and colon tissue was removed for the next analysis.

Sol-gel-derived-HAP

To prepare the nanoHAP, Ca $(NO_3)_2.4H_2O$ solution was prepared (0.01 mole dissolved in 20 ml ionized water, Ca sol). 0.62 mole of Tri-ethyl phosphate (TEP) was dissolved in 10 ml ionized water alongside slow addition of ethanol to the solution (P sol). Next, the obtained clear solution was kept at 35°C under stirring for a day and night for completion of the hydrolysis process. Next, P sol was added dropwise to the Ca sol. The initially recorded *p*H of the solution was 5 but the final one was regulated to 10 by NaOH (1M) and then was stirred for 1 hr at 60 °C. The final lemon-colored gel was aged for 2 days at 25 °C and next was dried at 100 °C for 1 day. In the end, the obtained white powder was calcined at 500 °C with thermal raising rate (2 °/min) for 2 hr (9).

Clinical and histopathological evaluations

Disease activity index (DAI) was determined as the total of the individual scores for bloody stools, stool quality, and BW loss, as previously described [8]. Up to the end of the research on day ten, all three parameters were reported daily. In brief, the scores were determined in accordance with Table 1. The colons were removed after sacrificing the mice on day 10 and the lengths and weights were recorded, the spleen was also harvested from the animals. The colon was opened and cut into longitudinally. For histopathological evaluations, the distal portion was obtained, and another half was snap-frozen for the next assays of oxidative stress. The colon tissue was then fixed and embedded in paraffin in a 10% formalin solution. Paraffin-embedded colon slides were stained with hematoxylin and eosin (H&E) and Masson trichrome (MT), and blinded histopathological scoring was performed based on Table 2, as described previously [10]. Images were taken using a light microscope (Olympus, Germany).

Measurement of oxidative stress markers

As an oxidant marker, malondialdehyde (MDA), and as anti-oxidant markers total thiol, Superoxide dismutase (SOD), and Catalase (CAT) activity were measured [11].

Statistical analysis

To perform statistical analysis, Graph Pad Prism software version 6.0 (Graph Pad Software Ltd, La Jolla, California, USA) was used. The outcomes were expressed as mean ± SEM. Using a one-way analysis of variance (ANOVA) followed by Tukey's

Table 2. Scoring parameters of colonic histological changes

Score	0	1	2	3	4
Inflammation	None	Mild	Moderate	Severe	
Mucosal damage	None	Mucus layer	Submucosa	Muscular and serosa	
Crypt loss	None	1/3	2/3	100%+intact epithelium	100% with epithelium lose
Pathological change range	None	1-25%	26-50%	51-75%	76-100%

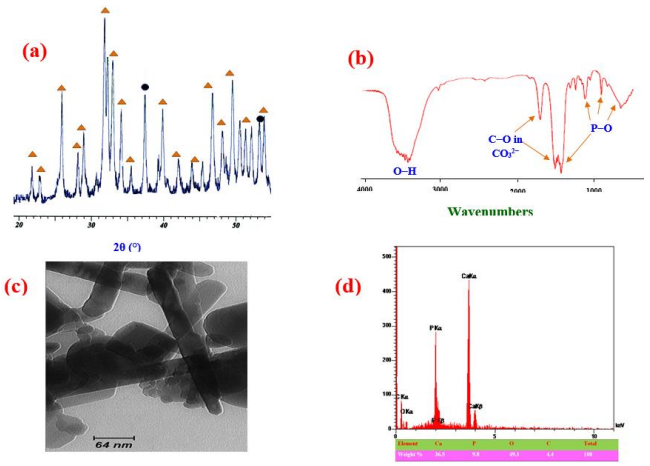

Fig. 2. XRD pattern (a), FTIR spectrum (b), TEM image (c), and (d) EDXA analysis of HAP (▲) calcined at 500 °C

post hoc, statistical differences between the groups were analyzed. The statistical difference was significant at $P<0.05$.

RESULTS

Characterization of synthesized HAP nanostructure

As mentioned in section 2.3, before mixing Ca and P sols, the hydrolysis process of P sol as an effective step was performed to achieve more completed future reactions. The hydrolysis step of TEP (eq. 1) results in the remarkable progress of polymerization and condensation reactions of Ca and P precursors (eq. 2) with the consequence of more purity of sol–gel-derived HAP product than the common methods [12, 13]. In order to prove the mentioned claim, the pH values of mixed sol before and after the aging process were recorded as ~ 6.4 and 3.9, respectively. This noted decreasing value emphasizes on more completed polymerization reaction of Ca and P moieties to make amorphous HAP (see eq. 2). Moreover, the disappearing of more Ca−P phases (like tri−calcium phosphate or pyrophosphate) as the secondary ones in the PXRD pattern confirmed the above conclusion (Fig. 2a).

$$OP(OEt)_3 + H_2O \rightarrow OP(OEt)_{3-x}(OH)_x + xC_2H_5OH \quad (1)$$

$$OP(OEt)_{3-x}(OH)_x + Ca^{2+} + NO_3^- \rightarrow (NO_3)^-(OH)–Ca–O–PO(OEt)_{3-x} + H^+ + C_2H_5OH + H_2O \quad (2)$$

The recorded PXRD pattern reveals the crystalization of HAP having the respected intense pertinent peaks (ICDD No.: 9-432) with hexagonal unit cell. These peaks can be assigned to the known different indices such as the main ones of (002), (210), and (211) (Fig. 2a). FT−IR spectrum is a helpful document to find the primary functional groups of the prepared HAP. The major bands of the spectrum that appeared at 480, 573, 972, and 1085–1215 cm^{-1} can be attributed to the stretching modes of phosphate, and the one recorded at 3365 cm^{-1} can be assigned to O–H functional groups (Fig. 2b). In addition, the stretching mode of C=O from $CO3^{2-}$ group outwarded in 1670 cm^{-1} shows the incorporation of carbonate species in apatite structure. However, entering carbonate ions in the nano−particle can improve the adsorption ability (DNA, protein, and so on) or catalytic activity of HAP. According to EDXA elemental analysis data and the measured Ca/P molar ratio as 2.17, $Ca_5(PO_4)_{2.3}(CO_3)_{1.6}(OH)$ formula can be suggested for this reported carbonated−HAP (see Fig. 1d). interestingly, the rod-like shape of HAp particle can be recognized in the TEM image. Finally, the particle size of HAP was measured in direct and indirect manners using TEM image and XRD pattern, respectively (Fig. 2a and 2c). Two obtained data showed the nearly same results with good consistency having the moderate particle size of 25−30 nm in width and 145−165 nm in length. The nano-particle size was evaluated with the aid of the Sherrer formula (eq. 3) [14, 15].

$$D = K\lambda / [W\cos(\theta)] \quad (3)$$

Where K is a constant value equal to (0.9), λ is the Cu Kα radiation (0.1544 nm), W is the full width at half-maximum, and θ is the diffraction angle (deg).

SSZ-HAP improved the Clinical and Macroscopic Features of Colitis

The initial clinical symptoms of mice colitis, for instance, BW loss, gross rectal bleeding, and

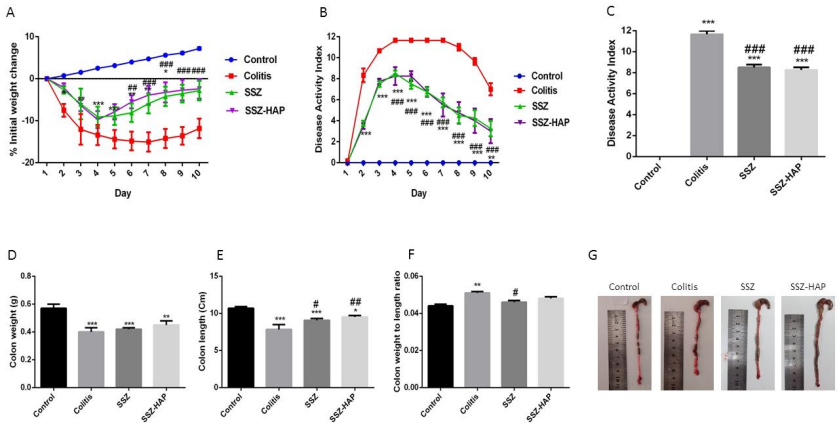

Fig. 3. Effect of SSZ-HAP on the pathology of dextran sodium sulfate (DSS)-induced experimental colitis. (A) % body weight change, (B) disease activity index (DAI) of controls, DSS, DSS-plus- SSZ, and DSS-plus- SSZ-HAP-treated mice, (C) colon length, (D) colon weight, (E) colon weight to length ratio, (F) macroscopic colon. Statistical significance among the groups was evaluated using one-way ANOVA followed by Tukey's post-test, where * P<0.05, **P<0.01, *** P<0.001 versus control, and # P<0.05, ## P<0.01, ### P<0.001 versus DSS. Data are expressed as a mean ± SEM (n = 6/group)

diarrhea were replicated by the administration of 1.5% DSS for 1 week. Until day 7, DSS-treated animals continuously decreased BW compared with controls (Fig. 3A). SSZ and SSZ-HAP successfully avoided BW loss in DSS-treated mice until Day 7 under these conditions. In DSS-treated mice, the DAI measured as a composite of occult fecal blood, stool consistency, and BW were substantially improved (P<0.001 both) from day 2 onwards (Fig. 3B). Treatment with SSZ and SSZ-HAP greatly decreased the incidence of disease symptoms, as shown by changes in fecal blood and watery stools from day 7 (both P<0.001) to day 10 (both P<0.001) compared with DSS-treated animals until the end of the research period. However, no significant differences in the clinical characteristics of colitis, such as BW change and DAI, between SSZ and SSZ-HAP were found in comparison with control, DSS-induced inflammation dramatically decreased colon length (Fig. 3C, P<0.001), colon weight (Fig. 3D, P<0.001), and colon weight to length ratio (Fig. 3E, P<0.01). SSZ-HAP therapy significantly (P<0.01) normalized the colon length as opposed to DSS-treated specimens, consistent with the decrease in disease incidence. No significant differences were detected between SSZ and SSZ-HAP in the macroscopic characteristics of colitis.

SSZ-HAP reduced inflammation and oxidative stress in acute colitis

Increased spleen weights are typically associated with the inflammation level. In contrast

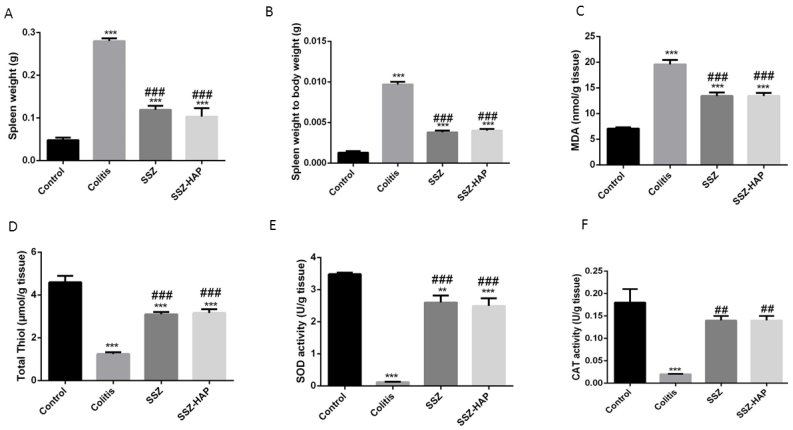

Fig. 4. Effect of SSZ-HAP on spleen damage and oxidative stress. (A) Spleen weight, (B) Spleen to body weight, (C) MDA, (D) Total thiol, (E) SOD activity, and (F) CAT activity. Statistical significance among the groups was evaluated using one-way ANOVA followed by Tukey's post-test, where * P<0.05, ** P<0.01, *** P<0.001 versus control, and # P<0.05, ## P<0.01, ### P<0.001 versus DSS. Data are expressed as a mean ± SEM (n = 6/group)

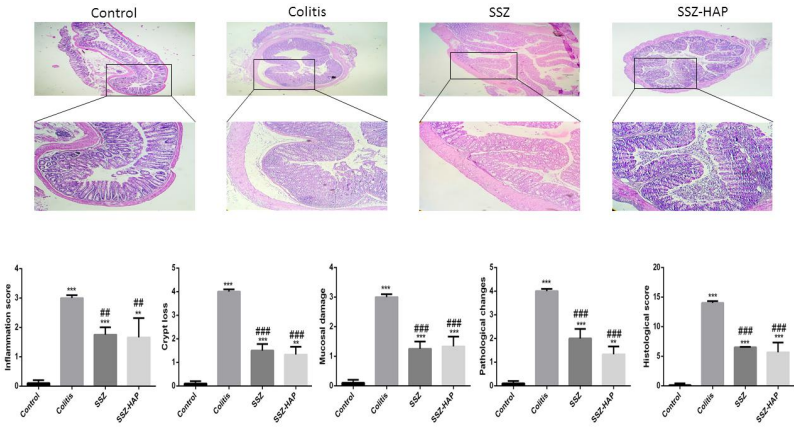

Fig. 5. Effect of SSZ-HAP on histopathology in DSS-induced colitis. (A) Histological representation of colon sections stained with H&E for the control group, DSS-treated mice and SSZ and SSZ-HAP treated mice at 4× and 10× magnification. (B-F) Histopathology scores for each animal were calculated after microscopic analysis of tissue sections from the proximal and distal colon. Statistical significance among groups was evaluated using one-way ANOVA followed by Tukey's post-test, where * P<0.05, ** P<0.01, *** P<0.001 versus control, and # P<0.05, ## P<0.01, ### P<0.001 versus DSS. Data are expressed as a mean ± SEM (n = 6/group)

with the control group, DSS induced an increase in spleen weight, with mean spleen weight and spleen weight to BW for DSS-only mice showing a significant difference compared with control mice (Fig 4A-B, P<0.001). Spleen weight and spleen to BW were also decreased by DSS in combination with SSZ or SSZ-HAP (Fig. 4A-B, P<0.001 both). Our findings also showed that SSZ and SSZ-HAP administration significantly increased total thiol, SOD, and CAT activity compared with DSS-treated mice, (Fig. 4D-F), while MDA levels decreased (Fig. 4C) in colitis mice (P<0.001 all). No significant differences were observed between SSZ and SSZ-HAP in the oxidative stress markers and spleen weight changes.

SSZ-HAP reduced the colon histopathology in acute colitis

Using H&E staining of tissue sections, the histopathology of the proximal and distal colon was analyzed (Fig. 5A). The integrity of colonic mucosal structures without signs of inflammation was demonstrated by colon tissues from the control group. In comparison, DSS-treated mice exhibited significant crypt degradation, loss of goblet cells, epithelial cell annihilation, submucosal edema, and massive inflammatory cell infiltration. In contrast to control, these DSS-induced improvements were correlated with higher cumulative histologic scores (Fig. 5B-F). SSZ-HAP therapy substantially improved colonic inflammation in DSS-treated mice

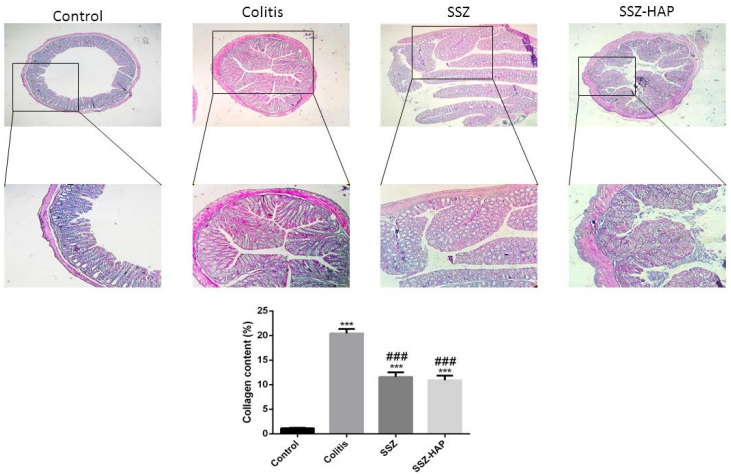

Fig. 6. Effect of SSZ-HAP on fibrosis in DSS-induced colitis. (A) Histological representation of colon sections stained with MT for the control group, DSS-treated mice and SSZ and SSZ-HAP treated mice at 4× and 10× magnification. (B) Percent of collagen content calculated after microscopic analysis of tissue sections with image J analysis software. Statistical significance among groups was evaluated using one-way ANOVA followed by Tukey's post-test, where * P<0.05, ** P<0.01, *** P<0.001 versus control, and # P<0.05, ## P<0.01, ### P<0.001 versus DSS. Data are expressed as a mean ± SEM (n = 6/group)

by preventing intestinal damage and significantly reducing the histologic score, but no significant differences were observed compared with SSZ alone (Fig. 5B-F). In comparison with its effect on colonic tissue, treatment with SSZ-HAP showed no significant protection for colonic tissue (Fig. 5).

SSZ-HAP reduced the colon fibrosis in acute colitis

Colonic tissues were stained with MT to assess the effect of SSZ-HAP on collagen deposition and fibrosis. Results showed that SSZ-HAP significantly decreased the deposition of collagen caused by DSS in colitis mice (Fig. 6A-B, $P<0.001$). Although, there was no significant difference between SSZ-HAP and SSZ groups.

DISCUSSION

Synthetic hydroxyapatite nanoparticles (HAP-NPs) are currently used in the field of Nanomedicine [16]. The effect on inflammation of nanoparticle size, chemistry, and charge is well studied [17-19]. However, there is still a limited understanding of the effect of nanoparticle morphology on the inflammatory response. The geometry of nanoparticles will influence how serum proteins and cell membrane receptors associate with particles, influencing cytotoxicity in turn [20]. Nanoparticle shape also strongly affects the rate of cellular uptake: rod-shaped particles are more readily internalized, accompanied by spheres and cones, whereas cubes are not easily internalized [21]. Differently shaped micro- [22] and nanoparticles [23, 24], are also affected by pro-inflammatory cytokines and ROS development, with needle morphology causing more inflammation than rods or spheres [25]. HAP-NPs morphology has been reported to influence ROS production and cell toxicity in other tissue and cell types [25-28].

The significant therapeutic ability of SSZ-HAP in reducing the incidence of DSS-induced disease by concurrently exercising both antioxidant and anti-inflammatory behaviors relative to SSZ alone is not shown by our findings. The current research used HAP-NPs that have been shown to be able to suppress proliferation and cause apoptosis in different cancer cells in recent years including osteosarcoma cells, [29] breast cancer cells [30], gastric cancer cells [31], colorectal cancer cells [32], and hepatic cancer cells [33] but spare the normal cells.

The use of SSZ can cause gastrointestinal-related adverse reactions such as loss of appetite, mild to severe diarrhea, and hair loss or thinness of the hair in patients [34], where no SSZ-HAP was observed in the present sample, while hair loss was observed with SSZ alone. SSZ and its HAP Nano form greatly enhanced BW, DAI, and histopathology, but no significant differences between SSZ and SSZ-HAP were found. Our observations confirm the previously documented participation of oxidative stress in disease pathogenesis and validate the usage of antioxidants to mitigate damage to structural tissue. It is well known that ROS are important signaling molecules involved in a multitude of physiological processes at low concentrations and over short periods of time [35]. However, as cells are subjected to elevated ROS levels and resulting lipid peroxidation for prolonged periods of time, they are unable to cope with oxidative damage in the digestive tract that can impair cell and tissue functions [36]. Therefore, it is believed that improving the machinery for antioxidant protection counteracts the dangerous acts of ROS in the body.

Total thiol, SOD, and CAT antioxidants remove free superoxide radicals directly to protect against lipid peroxidation [37, 38]. A significant increase in lipid peroxidation and decreased levels of antioxidant enzymes have been observed in prior studies of acute gut inflammation in the DSS model [39-41]. Significant reductions in MDA levels following SSZ therapy have been noted, with no significant difference between SSZ and SSZ-HAP [42]. SSZ and its Nano form increased the SOD activity rate in our sample, in line with the activation of an endogenous defense mechanism (Fig. 6).

Gut inflammation, along with altered barrier integrity and antioxidant response, is characterized by the overproduction of pro-inflammatory markers [43, 44]. The recruitment of lamina propria neutrophils and macrophages during mucosal injury results in inflammation by the aberrant release of pro-inflammatory markers cascades [45]. DSS-induced acute colitis is an inflammatory mouse model driven by macrophage/Th1/Th17 with elevated marker levels including TNF- α (a hallmark of DSS-induced inflammation), IL-6, IL-1, and IL-17 [46-48]. It is also assumed that inhibition of pro-inflammatory markers is an essential part of the therapeutic strategy toward UC. Our findings indicate that SSZ greatly suppresses inflammation, but its Nano form cannot significantly reduce

inflammation. The present research, to our knowledge, is the first to investigate the properties of HAP-NPs in acute colitis pathology. Considering the impact of HAP-NPs on gastrointestinal cancers, HAP-NPs are unable to decrease the symptoms of acute colitis.

CONCLUSION

Our results indicated that SSZ-HAP administration to DSS-treated mice attenuated acute inflammation in colon tissue and clinical signs/symptoms in colitis and this could be a good strategy for future studies on the use of nanoparticles with more anti-inflammatory effects such as zinc or Ag to improve the effectiveness of standard drugs in the treatment of colitis.

ACKNOWLEDGMENTS

Mashhad University of Medical Sciences, (grant No. 991285, Majid Khazaei) supported this study.

Conflicts of interest

The authors declare that they have no conflicts of interest.

REFERENCES

1. Baumgart DC, Carding SR. Inflammatory bowel disease: cause and immunobiology. The Lancet. 2007;369(9573):1627-40.
2. Biasi F, Leonarduzzi G, Oteiza PI, Poli G. Inflammatory bowel disease: mechanisms, redox considerations, and therapeutic targets. Antioxid Redox Signal. 2013;19(14):1711-1747.
3. Neurath MF. Current and emerging therapeutic targets for IBD. Nat. Rev. Gastroenterol. Hepatol. 2017;14(5):269-78.
4. Naeem M, Awan UA, Subhan F, Cao J, Hlaing SP, Lee J, et al. Advances in colon-targeted nano-drug delivery systems: challenges and solutions. Arch Pharm Res. 2020:1-17.
5. Hua S, Marks E, Schneider JJ, Keely S. Advances in oral nano-delivery systems for colon targeted drug delivery in inflammatory bowel disease: selective targeting to diseased versus healthy tissue. Nanomed.: Nanotechnol Biol Med. 2015;11(5):1117-1132.
6. Zhu S, Huang B, Zhou K, Huang S, Liu F, Li Y, et al. Hydroxyapatite nanoparticles as a novel gene carrier. J Nanopart Res. 2004;6(2):307-311.
7. Syamchand SS, Sony G. Multifunctional hydroxyapatite nanoparticles for drug delivery and multimodal molecular imaging. Microchimica Acta. 2015;182(9-10):1567-1589.
8. Asgharzadeh F, Hashemzadeh A, Yaghoubi A, Avan A, Nazari SE, Soleimanpour S, et al. Therapeutic effects of silver nanoparticle containing sulfasalazine on DSS-induced colitis model. J Drug Deliv Sci Technol. 2020;121(9-10):1257-1269.
9. Kadu K, Tripathi R, Kowshik M, Ramanan SR. Morphological Evolution of Hydroxyapatite Nanoparticles, Synthesized via Modified Sol-Gel and Microemulsion Technique, in Response to Their Synthesis Microenvironment. Crystal Res and Technol. 2022;114(4-9):1245-1251.
10. Rahmani F, Asgharzadeh F, Avan A, Barneh F, Parizadeh MR, Ferns GA, et al. Rigosertib potently protects against colitis-associated intestinal fibrosis and inflammation by regulating PI3K/AKT and NF-κB signaling pathways. Life Sci. 2020:117(4-7):1114-1121.
11. Bargi R, Asgharzadeh F, Beheshti F, Hosseini M, Sadeghnia HR, Khazaei M. The effects of thymoquinone on hippocampal cytokine level, brain oxidative stress status and memory deficits induced by lipopolysaccharide in rats. Cytokine. 2017; 96:173-184.
12. Cheng K, Weng W, Han G, Du P, Shen G, Yang J, et al. The effect of triethanolamine on the formation of sol–gel derived fluoroapatite/hydroxyapatite solid solution. Mater. Chem. Phys. 2003;78(3):767-771.
13. Liu D-M, Troczynski T, Tseng WJ. Water-based sol–gel synthesis of hydroxyapatite: process development. Biomaterials. 2001;22(13):1721-1730.
14. Vakili SN, Rezayi M, Chahkandi M, Meshkat Z, Fani M, Moattari A. A novel electrochemical DNA biosensor based on hydroxyapatite nanoparticles to detect BK polyomavirus in the urine samples of transplant patients. IEEE Sens J. 2020;20(20):12088-95.
15. Weibel A, Bouchet R, Boulc' F, Knauth P. The big problem of small particles: a comparison of methods for determination of particle size in nanocrystalline anatase powders. Chem. Mater. 2005;17(9):2378-2385.
16. Verma G, Shetake NG, Pandrekar S, Pandey B, Hassan P, Priyadarsini K. Development of surface functionalized hydroxyapatite nanoparticles for enhanced specificity towards tumor cells. Eur J Pharm Sci. 2020; 144:105206.
17. Ai J, Biazar E, Jafarpour M, Montazeri M, Majdi A, Aminifard S, et al. Nanotoxicology and nanoparticle safety in biomedical designs. Int. J. Nanomedicine. 2011; 6:1117.
18. Guildford A, Poletti T, Osbourne L, Di Cerbo A, Gatti A, Santin M. Nanoparticles of a different source induce different patterns of activation in key biochemical and cellular components of the host response. J R Soc Interface. 2009;6(41):1213-1221.
19. Yang H, Liu C, Yang D, Zhang H, Xi Z. Comparative study of cytotoxicity, oxidative stress and genotoxicity induced by four typical nanomaterials: the role of particle size, shape and composition. J Appl Toxicol. 2009;29(1):69-78.
20. Albanese A, Tang PS, Chan WC. The effect of nanoparticle size, shape, and surface chemistry on biological systems. Annu. Rev. Biomed. Eng. 2012; 14:1-16.
21. Gratton SE, Ropp PA, Pohlhaus PD, Luft JC, Madden VJ, Napier ME, et al. The effect of particle design on cellular internalization pathways. Proc. Natl. Acad. Sci. 2008;105(33):11613-11618.
22. Laquerriere P, Grandjean-Laquerriere A, Jallot E, Balossier G, Frayssinet P, Guenounou M. Importance of hydroxyapatite particles characteristics on cytokines production by human monocytes in vitro. Biomaterials. 2003;24(16):2739-2747.
23. Huang J, Best S, Bonfield W, Brooks R, Rushton N, Jayasinghe S, et al. In vitro assessment of the biological response to nano-sized hydroxyapatite. J. Mater. Sci.: Mater. Med. 2004;15(4):441-445.
24. Lee JH, Ju JE, Kim BI, Pak PJ, Choi EK, Lee HS, et al. Rod-shaped iron oxide nanoparticles are more toxic than sphere-shaped nanoparticles to murine macrophage cells. Environ. Toxicol. Chem. 2014;33(12):2759-2766.
25. Zhao X, Ng S, Heng BC, Guo J, Ma L, Tan TTY, et al. Cytotoxicity of hydroxyapatite nanoparticles is shape and cell dependent. Arch Toxicol. 2013;87(6):1037-1052.
26. Fan Q, Wang YE, Zhao X, Loo JS, Zuo YY. Adverse biophysical effects of hydroxyapatite nanoparticles on natural

pulmonary surfactant. ACS nano. 2011;5(8):6410-6416.
27. Tay CY, Fang W, Setyawati MI, Chia SL, Tan KS, Hong CHL, et al. Nano-hydroxyapatite and nano-titanium dioxide exhibit different subcellular distribution and apoptotic profile in human oral epithelium. ACS Appl Mater Interfaces. 2014;6(9):6248-6256.
28. Zhao X, Ong KJ, Ede JD, Stafford JL, Ng KW, Goss GG, et al. Evaluating the toxicity of hydroxyapatite nanoparticles in catfish cells and zebrafish embryos. Small. 2013;9(9-10):1734-1741.
29. Shi Z, Huang X, Cai Y, Tang R, Yang D. Size effect of hydroxyapatite nanoparticles on proliferation and apoptosis of osteoblast-like cells. Acta Biomater. 2009;5(1):338-345.
30. Jin J, Zuo G, Xiong G, Luo H, Li Q, Ma C, et al. The inhibition of lamellar hydroxyapatite and lamellar magnetic hydroxyapatite on the migration and adhesion of breast cancer cells. J Mater Sci Mater Med. 2014;25(4):1025-1031.
31. Chen X, Deng C, Tang S, Zhang M. Mitochondria-dependent apoptosis induced by nanoscale hydroxyapatite in human gastric cancer SGC-7901 cells. Biol Pharm Bull. 2007;30(1):128-132.
32. Dey S, Das M, Balla VK. Effect of hydroxyapatite particle size, morphology and crystallinity on proliferation of colon cancer HCT116 cells. Mater Sci Eng C. 2014; 39:336-339.
33. Ezhaveni S, Yuvakkumar R, Rajkumar M, Sundaram NM, Rajendran V. Preparation and characterization of nano-hydroxyapatite nanomaterials for liver cancer cell treatment. Nanosci Nanotechnol. 2013;13(3):1631-1638.
34. Di Prospero NA, Sumner CJ, Penzak SR, Ravina B, Fischbeck KH, Taylor JP. Safety, tolerability, and pharmacokinetics of high-dose idebenone in patients with Friedreich ataxia. Arch Neurol. 2007;64(6):803-808.
35. Bhattacharyya A, Chattopadhyay R, Mitra S, Crowe SE. Oxidative stress: an essential factor in the pathogenesis of gastrointestinal mucosal diseases. Physiol Rev. 2014;94(2):329-354.
36. Tian T, Wang Z, Zhang J. Pathomechanisms of oxidative stress in inflammatory bowel disease and potential antioxidant therapies. Oxid Med Cell Longev. 2017;2017.
37. Siegel D, Gustafson DL, Dehn DL, Han JY, Boonchoong P, Berliner LJ, et al. NAD (P) H: quinone oxidoreductase 1: role as a superoxide scavenger. Mol Pharmacol. 2004;65(5):1238-1247.
38. Zhu H, Jia Z, Mahaney JE, Ross D, Misra HP, Trush MA, et al. The highly expressed and inducible endogenous NAD (P) H: quinone oxidoreductase 1 in cardiovascular cells acts as a potential superoxide scavenger. Cardiovasc Toxicol. 2007;7(3):202-211.
39. Nam ST, Hwang JH, Kim DH, Park MJ, Lee IH, Nam HJ, et al. Role of NADH: quinone oxidoreductase-1 in the tight junctions of colonic epithelial cells. BMB Rep. 2014;47(9):494-499.
40. Pandurangan AK, Mohebali N, Norhaizan ME, Looi CY. Gallic acid attenuates dextran sulfate sodium-induced experimental colitis in BALB/c mice. Drug Des Devel Ther. 2015; 9:3923.
41. Shafik NM, Gaber RA, Mohamed DA, Ebeid AM. Hesperidin modulates dextran sulfate sodium-induced ulcerative colitis in rats: Targeting sphingosine kinase-1- sphingosine 1 phosphate signaling pathway, mitochondrial biogenesis, inflammation, and apoptosis. J Biochem Mol Toxicol. 2019;33(6):27.
42. Mellors A, Tappel AL. The inhibition of mitochondrial peroxidation by ubiquinone and ubiquinol. J Biol Chem. 1966;241(19):4353-4356.
43. Rao R. Oxidative stress-induced disruption of epithelial and endothelial tight junctions. Front Biosci. 2008; 13:7210-26.
44. Strober W, Fuss IJ. Proinflammatory cytokines in the pathogenesis of inflammatory bowel diseases. Gastroenterology. 2011;140(6):1756-1767.
45. Geremia A, Biancheri P, Allan P, Corazza GR, Di Sabatino A. Innate and adaptive immunity in inflammatory bowel disease. Autoimmun Rev. 2014;13(1):3-10.
46. Alex P, Zachos NC, Nguyen T, Gonzales L, Chen TE, Conklin LS, et al. Distinct cytokine patterns identified from multiplex profiles of murine DSS and TNBS-induced colitis. Inflamm Bowel Dis. 2009;15(3):341-352.
47. Neurath MF. Cytokines in inflammatory bowel disease. Nat Rev Immunol. 2014;14(5):329-342.
48. Strober W, Fuss IJ, Blumberg RS. The immunology of mucosal models of inflammation. Annu Rev Immunol. 2002; 20:495-549.